doi:10.1016/j.jmb.2005.12.082 J. Mol. Biol. (2006) 357, 358–364

JMB

Available online at www.sciencedirect.com

SCIENCE DIRECT®

ELSEVIER

COMMUNICATION

Crystal Structure of RAIDD Death Domain Implicates Potential Mechanism of PIDDosome Assembly

Hyun Ho Park and Hao Wu*

Department of Biochemistry Weill Medical College and Graduate School of Medical Sciences of Cornell University New York, NY 10021, USA

*Corresponding author

Caspase-2 is implicated in stress-induced apoptosis that acts as an upstream initiator of mitochondrial permeabilization. Recent studies have shown that caspase-2 activation requires a molecular complex known as the PIDDosome comprising the p53-inducible protein PIDD, the adapter protein RAIDD and caspase-2. RAIDD has an N-terminal caspase recruitment domain (CARD) that interacts with the CARD of caspase-2 and a C-terminal death domain (DD) that interacts with the DD in PIDD. As a first step towards elucidating the molecular mechanisms of caspase-2 activation, we report the crystal structure of RAIDD DD at 2.0 Å resolution. The high-resolution structure reveals important features of RAIDD DD that may be important for DD folding and dynamics and for assembly of the PIDDosome.

Keywords: crystal structure; death domain; apoptosis; RAIDD; PIDDosome

Apoptosis plays a critical role in normal development, immune responses and tissue homeostasis, whereas its malfunction is related to many human diseases, including cancer, degenerative disorders, and autoimmunity.[1,2] The execution of apoptosis is performed by caspases, a family of cysteine proteases that cleave specifically after Asp residues.[3,4] Caspases are synthesized as single-chain zymogens and require a highly regulated process for their activation. On the basis of their roles in apoptosis, caspases are divided into initiator caspases such as caspase-2, caspase-8, caspase-9 and caspase-10, and effector caspases such as caspase-3 and caspase-7. Initiator caspases are activated and auto-processed by recruitment to oligomeric signaling complexes. In contrast, effector caspases are activated upon cleavage by initiator caspases.

There are two classical pathways of initiator caspase activation and apoptosis.[5] Cells that are damaged or neglected undergo apoptosis through a mitochondria-dependent pathway known as the intrinsic pathway, which results in the activation of caspase-9. On the other hand, stimulation of caspase activity in healthy but unwanted or potentially dangerous cells can be achieved through cell surface death receptors, which are members of the tumor necrosis factor receptor superfamily. Death receptor-mediated cell death forms the extrinsic apoptosis pathway that results in the activation of caspase-8 and -10.[6,7] These receptors contain a death domain (DD) in their intracellular regions.[8–10] For Fas, a prototypical member of death receptors, its DD recruits the Fas-associated death domain (FADD) adaptor protein *via* a homotypic interaction with the C-terminal DD of FADD.[11,12] FADD also contains an N-terminal death effector domain that interacts homotypically with the tandem death effector domains in the pro-domains of caspase-8 or -10.[13,14] These interactions form the ternary death-inducing signaling complex (DISC) containing Fas, FADD and caspase-8 or caspase-10. Both pathways further activate effector caspases that cleave downstream targets such as DFF45 to perform the apoptotic program.

Recent studies have shown that genotoxic stress activates an equally or more important apoptosis pathway that results in the activation of the initiator caspase, caspase-2, the most evolutionarily conserved caspase.[15–17] This pathway may function upstream of the mitochondria in the intrinsic apoptosis pathway by controlling the release of

Abbreviations used: DD, death domain; FADD, Fas-associated death domain; DISC, death-inducing signaling complex; CARD, caspase recruitment domain; PIDD, p53-induced protein with a death domain; RAIDD, RIP-associated ICH-1 homologous protein with a death domain; RIP, RIP the DD-containing Ser/Thr kinase involved in tumor necrosis factor signaling.

E-mail address of the corresponding author: haowu@med.cornell.edu

cytochrome *c* and other apoptogenic factors. Caspase-2 has a caspase recruitment domain (CARD) at its amino-terminal region. Activation of caspase-2 appears to require a large oligomeric molecular complex known as the PIDDosome that contains PIDD (p53-induced protein with a death domain), RAIDD (RIP-associated ICH-1 homologous protein with a death domain) and caspase-2.[18–20] RAIDD was identified originally as a protein associated with RIP, the DD-containing Ser/Thr kinase involved in tumor necrosis factor signaling.[21] It has both an N-terminal CARD and a C-terminal DD, and acts as a bridge between caspase-2 and PIDD. While PIDD and RAIDD interact with each other *via* their DDs, RAIDD and caspase-2 interact with each other *via* their CARDs. Given the important function of caspase-2, it is crucial to elucidate the molecular basis of its activation through structural studies.

DDs are versatile protein interaction modules, which, together with death effector domains, CARDs, and Pyrin domains, comprise the DD superfamily,[22,23] one of the biggest families of protein domains. DDs exhibit the six helix bundle structural fold and are highly prevalent in apoptotic and other signaling proteins.[23] Here, we report the crystal structure of RAIDD DD at 2.0 Å resolution. The structure revealed new and interesting aspects of DD folding and dynamics, and implicated conserved surface residues in RAIDD DD for PIDD and RIP interaction, and PIDDosome assembly.

RAIDD DD structure and surface salt-bridges

The high-resolution structure of RAIDD DD (Figures 1 and 2; Table 1) showed that it comprises seven helices, H0 to H6, out of which helices H1 to H6 form the canonical anti-parallel six-helix bundle fold characteristic of the DD superfamily. The N and C termini of RAIDD DD are at the same side of the molecule. With the exception of H0, residues from all helices contribute to the formation of the hydrophobic core; H0 is therefore unlikely to be an integral part of the RAIDD DD. In addition to the helices, the H1-H2 and H2-H3 loops contribute residues to the structural core. In contrast, the remaining loops, H3-H4, H4-H5 and H5-H6 are much more exposed. Residues buried within the core of RAIDD DD are almost all hydrophobic. They are conserved among RAIDD DDs from different species (Figure 2).

There are several side-chain hydrogen bonding interactions on the surface of RAIDD DD that may be important for the precise orientations of the helices (Figure 1(c)). One such interaction is the salt-bridge between E132 of H2 and K149 of H3. Another salt-bridge exists between D144 of H3 and R170 of H4. There are two hydrogen bonding pairs, between Q125 of H1 and Q157 of H4, and between Q178 and N182 of H5. Additionally, a hydrogen bonding network exists between H3 and H4, involving residues N151, H152, N155, S158 and E162. Interestingly, no surface hydrogen bonding interactions exists between residues in helices H0, H5 or H6 and those in the remaining part of the structure.

Among these hydrogen bonding and salt-bridge interactions, residues involved in the ion pairs of E132-K149 and D144-R170 are highly conserved among RAIDD DDs from different species (Figure 2). This suggests that they play an important role in DD folding and stability. E132 is almost identical among RAIDD DDs and K149 is conserved as Lys and Arg. The only exception is in RAIDD from zebra fish, in which E132 and K149 are both replaced by different residues, Lys and Cys, respectively. D144 and R170 are identical among ten and nine of the 11 aligned sequences, respectively. In *Xenopus laevis*, R170 is replaced by Gln, which could still possibly form hydrogen bonds with D144. In puffer fish, D144 is replaced by Ala and R170 is replaced by Gly. Similarly, surface salt-bridge interactions are important for the stability of coiled-coil structures such as GCN4.[24]

B-factor distribution and potential dynamic properties of RAIDD DD

The structure of RAIDD DD is highly compact and ordered with an average *B*-factor of 32.0 Å^2 (Table 1). Plotting individual *B*-factors for each residue along the protein sequence (Figure 2) showed that the middle portion of the structure, including H1, H2, H3 and H4, has the lowest *B*-factors. The two ends of the sequence, including helices H0, H5 and H6, are more flexible with higher *B*-factors. This trend in *B*-factor distribution may be consistent with the lack of further polar interactions between these helices and the remaining part of the structure to precisely tie down these regions of the structure (Figure 1(c)).

Residues that are buried in the hydrophobic core tend to have lower *B*-factors, in their main chains and in their side-chains (Figure 2). In contrast, the more exposed residues may have low main-chain *B*-factors, but often have higher side-chain *B*-factors. The ends of the structures, H0 and H6, have both higher main-chain and higher side-chain *B*-factors. However, in the context of full-length RAIDD, in which H0 is not the natural N terminus of the molecule, this situation may be somewhat different. For RAIDD DD, the crystal packing does not seem to have influenced the *B*-factor distribution significantly, as there is no observed trend of a lower average *B*-factor in residues involved in crystal packing (Figure 2).

Differences with FADD DD structure

On the molecular level, the closest functional homologue of RAIDD is FADD, the adapter protein involved in the assembly of the DISC for extrinsic cell death. Both RAIDD and FADD are bipartite adapter proteins that use their C-terminal DDs and N-terminal domains to assemble ternary complexes

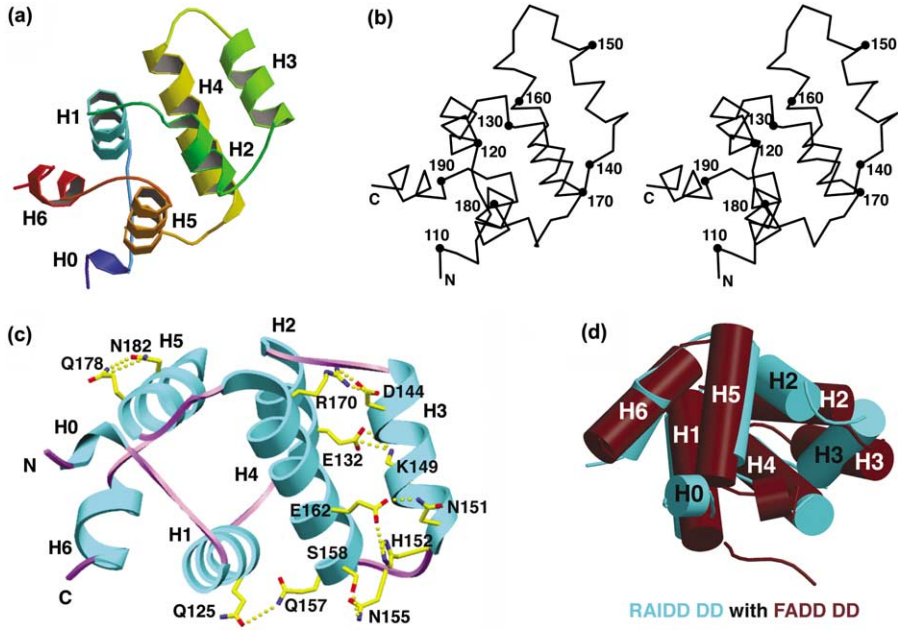

Figure 1. Crystal structure of RAIDD DD. (a) Ribbon diagram of RAIDD DD. The chain from N terminus to C terminus is colored by the spectrum from blue to red. Helices are labeled. (b) Stereo C^{α} trace of RAIDD DD structure. Residue numbers for every tenth residue are labeled. (c) Intra-molecular surface hydrogen bonding interactions. Helices are labeled and residues involved in these interactions are shown. (d) Superposition of RAIDD DD (cyan) with FADD DD (dark red). Helices in FADD DD are labeled in white and those in RAIDD DD in black. Only H0, H2 and H3 of RAIDD DD are labeled to show the differences with FADD DD.

in caspase activation. Despite the functional similarity, RAIDD DD shows large structural differences in comparison with FADD DD. In particular, helices H2 and H3 of RAIDD DD show dramatic differences in orientations (Figure 1(d)). Additional conspicuous differences are at the loops connecting the helices, especially those at H3-H4 (Figures 1(d) and 2).

In contrast to the more charged nature of FADD DD, the RAIDD DD surface is much more hydrophobic (Figure 3(b)). This is the case for both sides of the molecule. Because DDs are protein interaction modules, their surface features dictate their mode of interactions with partners. In the case of FADD DD, although no direct structural information is available, it has been suggested that its charged surface is important for interaction with Fas.[25,26] In the only structure of a DD complex, between the *Drosophila* proteins Pelle and Tube,[27] the interaction is mixed, with both hydrophobic and hydrophilic components. In the only other known structure of a complex within the DD superfamily, the Apaf-1/caspase-9 CARD complex, the interaction is mediated largely by charge complementarity.[28] The more hydrophobic surface may have functional significance in assembling the PIDDosome for caspase-2 activation (see below).

Conserved surface of RAIDD DD: potential PIDD and RIP interaction site

Besides residues that are either buried in the hydrophobic core or participate in surface hydrogen bonding interactions, a number of residues are conspicuously conserved among RAIDD DDs from different species (Figure 2). These include I110, L136, Y146, V156, V161, I165 and L198, which, without exception, are conserved as large hydrophobic residues on the surface of RAIDD DD. In addition to hydrophobic residues, four charged residues, R126, E130, R147 and E188, are absolutely conserved among different RAIDD species.

Mapping of these residues onto the RAIDD DD surface shows that they occupy one side of the hydrophobic surface and extend to the surrounding more charged region (Figure 3). In contrast, the other side of the hydrophobic surface does not have any of these conserved residues (Figure 3(c), lower left panel). The mapping analysis suggests that this extensive surface of RAIDD DD, comprising both a hydrophobic central region and a more charged peripheral region, may be involved in interaction with PIDD and RIP.

Because RAIDD DD is involved in the assembly of the oligomeric PIDDosome, it is possible that this mapped region of the RAIDD DD surface interacts with multiple molecules of PIDD or RIP. In addition, although RAIDD DD is a monomer in solution, it may self-associate in the context of the PIDDosome. Therefore, these conserved residues may be involved in this self-association as well.

In the case of FADD DD, residues in H2 and H3 helices were shown to be important for Fas interaction.[25] This is also the region where RAIDD DD shows dramatic structural differences from FADD DD. Subsequently, an extensive surface of

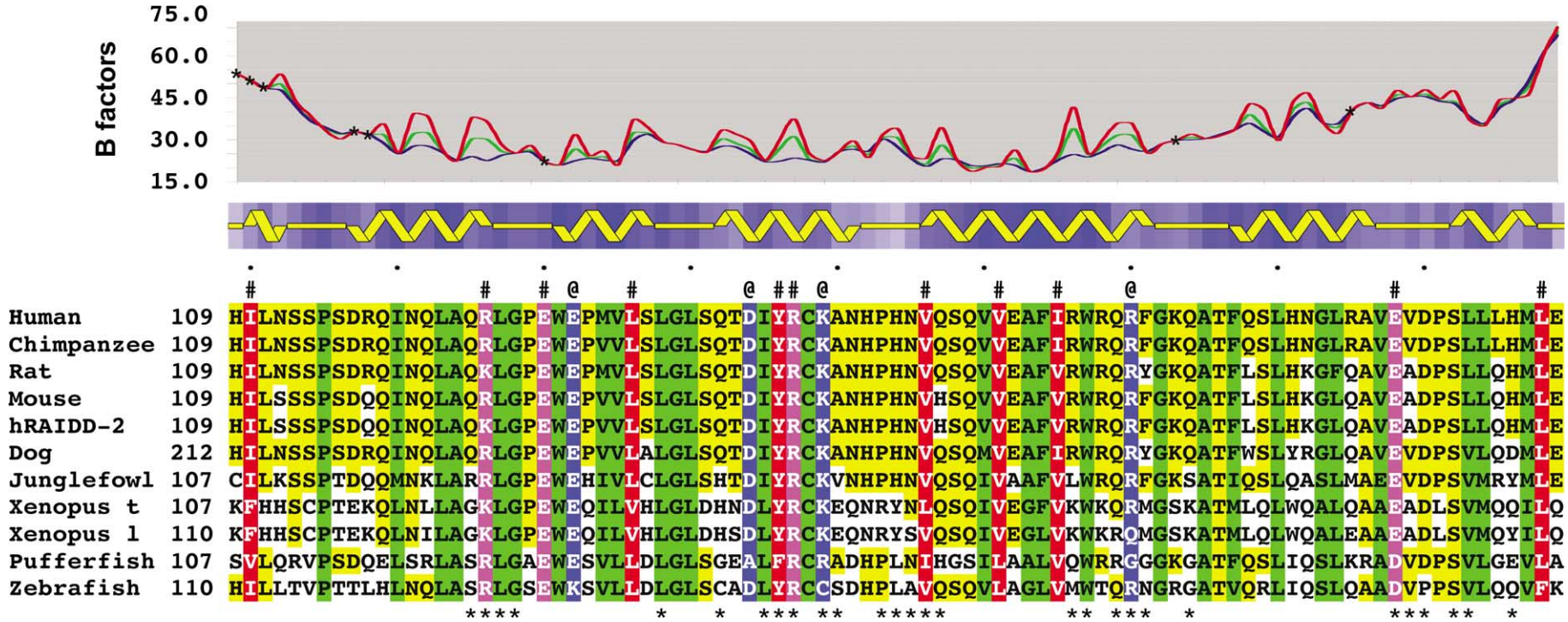

Figure 2. Structure-based sequence alignment of RAIDD DD from different species. hRAIDD-2, RAIDD-related protein from human; Xenopus l, *Xenopus laevis*; Xenopus t, *Xenopus tropicalis*. Sequence identities between human RAIDD DD and those from other species in this Figure range from 42% to 98%. Secondary structures (helices H0 to H6) are shown above the sequences and surface area burials are shown as dark and light blue boxes for buried and more exposed residues, respectively. Residues at the hydrophobic core are shaded in green; those that are involved in surface salt-bridges (labeled as @) are shaded in blue; conserved exposed hydrophobic and charged residues (labeled as #) are shaded in red and magenta, respectively; and remaining residues identical with human RAIDD are shaded in yellow. Residues involved in crystal packing interactions are labeled as *. Average main chain (blue line), side-chain (red line) and whole residue (green line) *B*-factors are plotted. An asterisk (*) on the plot denotes residues with disordered side-chains.

Table 1. Crystallographic statistics

	Se-Met	Native
A. *Data collection*		
Space group	$P3_121$	$P3_121$
Cell dimensions		
a (Å)	56.3	56.1
b (Å)	56.3	56.1
c (Å)	64.9	64.9
Resolution (Å)	50–2.0	50–2.0
R_{sym}[a] (%)	6.2 (27.4)	5.5 (17.9)
$I/\sigma I$[a]	61.8 (13.5)	43.9 (17.5)
Completeness[a] (%)	100.0 (100.0)	99.7 (99.8)
Redundancy[a]	11.0 (10.6)	8.9 (8.9)
B. *Refinement*		
Resolution (Å)		50–2.0
Reflections used (completeness, %)		8063 (96.9)
R_{work} (%)		23.1
R_{free} (%)		24.1
No. atoms		
Protein		704
Water and other small molecules		55
Average *B*-factors		
Protein (Å^2)		32.0
Water and other small molecules (Å^2)		40.4
r.m.s deviations		
Bond lengths (Å)		0.005
Bond angles (deg.)		1.0
Ramachandran plot		
Most favored regions (%)		91.3
Additionally allowed regions (%)		8.7

Human RAIDD DD was expressed in *Escherichia coli* under overnight induction at 20 °C. The protein contained a carboxyl terminal His-tag and was purified by nickel affinity chromatography and gel-filtration chromatography. The protein was concentrated to 4–6 mg/ml and crystallized using the hanging-drop, vapor-diffusion method. The reservoir contained 2 M Na/K phosphate at pH 7. Selenomethionine-substituted RAIDD DD was produced as described,[30] and crystallized similarly. The crystals diffracted to 2.0 Å spacing under synchrotron radiation. They belong to space group $P3_121$ with one molecule per crystallographic asymmetric unit. A single-wavelength anomalous diffraction (SAD) data set was collected at the selenium peak wavelength ($E=12664$ eV, $\lambda=0.979$ Å) at the X4A beamline of National Synchrotron Light Source (NSLS) using a Quantum 4 CCD detector. Data processing and scaling was carried out in the HKL2000 package.[31] A native data set was collected and used for model refinement. Phase calculation and phase improvement were performed at a resolution of 2.0 Å using the programs SOLVE and RESOLVE.[32] Approximately 80% of the structure was auto-traced. Model building and refinement were performed in O[33] and CNS,[34] respectively. The final atomic model contains residues 109–199. Ribbon diagrams were generated using the programs Setor[35] and MOLSCRIPT/Raster3D,[36,37] and molecular surface representations were produced with the program GRASP.[38]

[a] The value for the highest resolution shell is shown in parentheses.

FADD DD that includes residues from all six helices was shown to participate in assembly of the DISC.[29] In RAIDD DD, the conserved surface residues are distributed in many regions of the protein sequence, but do not appear to be as extensive as the situation for FADD DD. It is possible that assembly of the DISC and the PIDDosome may be quite different in detail, including stoichiometry, nature of the inter-

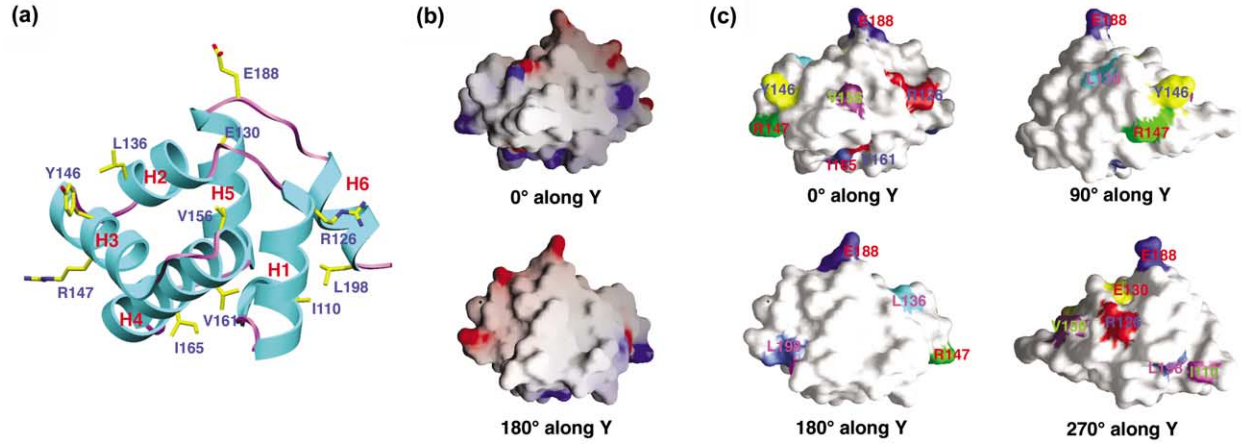

Figure 3. Mapping of conserved exposed residues onto RAIDD DD. (a) Ribbon diagram of RAIDD DD with conserved surface residues. (b) Electrostatic surface representation of RAIDD DD. Two orientations are shown. (c) Molecular surface representation of RAIDD DD with conserved exposed residues colored and labeled. Four orientations of RAIDD DD surface are shown.

face and region of the molecular surface. In summary, the structure of RAIDD DD provides a first step towards elucidating the molecular basis of caspase-2 activation.

Acknowledgements

We thank Randy Abramowitz and John Schwanof for use of the X4A beamline at NSLS. This work was supported by the National Institute of Health (R01 AI-50872).

References

1. Rathmell, J. C. & Thompson, C. B. (2002). Pathways of apoptosis in lymphocyte development, homeostasis, and disease. *Cell*, **109**, S97–S107.
2. Thompson, C. B. (1995). Apoptosis in the pathogenesis and treatment of disease. *Science*, **267**, 1456–1461.
3. Salvesen, G. S. (2002). Caspases and apoptosis. *Essays Biochem.* **38**, 9–19.
4. Riedl, S. J. & Shi, Y. (2004). Molecular mechanisms of caspase regulation during apoptosis. *Nature Rev. Mol. Cell. Biol.* **5**, 897–907.
5. Danial, N. N. & Korsmeyer, S. J. (2004). Cell death: critical control points. *Cell*, **116**, 205–219.
6. Lavrik, I., Golks, A. & Krammer, P. H. (2005). Death receptor signaling. *J. Cell Sci.* **118**, 265–267.
7. Peter, M. E. & Krammer, P. H. (2003). The CD95(APO-1/Fas) DISC and beyond. *Cell Death Differ.* **10**, 26–35.
8. Itoh, N. & Nagata, S. (1993). A novel protein domain required for apoptosis. Mutational analysis of human Fas antigen. *J. Biol. Chem.* **268**, 10932–10937.
9. Tartaglia, L. A., Ayres, T. M., Wong, G. H. & Goeddel, D. V. (1993). A novel domain within the 55 kd TNF receptor signals cell death. *Cell*, **74**, 845–853.
10. Wajant, H. (2002). The Fas signaling pathway: more than a paradigm. *Science*, **296**, 1635–1636.
11. Kischkel, F. C., Hellbardt, S., Behrmann, I., Germer, M., Pawlita, M., Krammer, P. H. & Peter, M. E. (1995). Cytotoxicity-dependent APO-1 (Fas/CD95)-associated proteins form a death-inducing signaling complex (DISC) with the receptor. *EMBO J.* **14**, 5579–5588.
12. Chinnaiyan, A. M., O'Rourke, K., Tewari, M. & Dixit, V. M. (1995). FADD, a novel death domain-containing protein, interacts with the death domain of Fas and initiates apoptosis. *Cell*, **81**, 505–512.
13. Muzio, M., Chinnaiyan, A. M., Kischkel, F. C., O'Rourke, K., Shevchenko, A., Ni, J. *et al.* (1996). FLICE, a novel FADD-homologous ICE/CED-3-like protease, is recruited to the CD95 (Fas/APO-1) death-inducing signaling complex. *Cell*, **85**, 817–827.
14. Boldin, M. P., Goncharov, T. M., Goltsev, Y. V. & Wallach, D. (1996). Involvement of MACH, a novel MORT1/FADD-interacting protease, in Fas/APO-1- and TNF receptor-induced cell death. *Cell*, **85**, 803–815.
15. Zhivotovsky, B. & Orrenius, S. (2005). Caspase-2 function in response to DNA damage. *Biochem. Biophys. Res. Commun.* **331**, 859–867.
16. Lassus, P., Opitz-Araya, X. & Lazebnik, Y. (2002). Requirement for caspase-2 in stress-induced apoptosis before mitochondrial permeabilization. *Science*, **297**, 1352–1354.
17. Wang, L., Miura, M., Bergeron, L., Zhu, H. & Yuan, J. (1994). Ich-1, an Ice/ced-3-related gene, encodes both positive and negative regulators of programmed cell death. *Cell*, **78**, 739–750.
18. Tinel, A. & Tschopp, J. (2004). The PIDDosome, a protein complex implicated in activation of caspase-2 in response to genotoxic stress. *Science*, **304**, 843–846.
19. Lin, Y., Ma, W. & Benchimol, S. (2000). Pidd, a new death-domain-containing protein, is induced by p53 and promotes apoptosis. *Nature Genet.* **26**, 122–127.
20. Duan, H. & Dixit, V. M. (1997). RAIDD is a new 'death' adaptor molecule. *Nature*, **385**, 86–89.
21. Hsu, H., Huang, J., Shu, H. B., Baichwal, V. & Goeddel, D. V. (1996). TNF-dependent recruitment of the protein kinase RIP to the TNF receptor-1 signaling complex. *Immunity*, **4**, 387–396.
22. Kohl, A. & Grutter, M. G. (2004). Fire and death: the pyrin domain joins the death-domain superfamily. *C. R. Biol.* **327**, 1077–1086.
23. Reed, J. C., Doctor, K. S. & Godzik, A. (2004). The domains of apoptosis: a genomics perspective. *Sci. STKE*, **2004**, re9.
24. Spek, E. J., Bui, A. H., Lu, M. & Kallenbach, N. R. (1998). Surface salt bridges stabilize the GCN4 leucine zipper. *Protein Sci.* **7**, 2431–2437.
25. Jeong, E. J., Bang, S., Lee, T. H., Park, Y. I., Sim, W. S. & Kim, K. S. (1999). The solution structure of FADD death domain. Structural basis of death domain interactions of Fas and FADD. *J. Biol. Chem.* **274**, 16337–16342.
26. Berglund, H., Olerenshaw, D., Sankar, A., Federwisch, M., McDonald, N. Q. & Driscoll, P. C. (2000). The three-dimensional solution structure and dynamic properties of the human FADD death domain. *J. Mol. Biol.* **302**, 171–188.
27. Xiao, T., Towb, P., Wasserman, S. A. & Sprang, S. R. (1999). Three-dimensional structure of a complex between the death domains of Pelle and Tube. *Cell*, **99**, 545–555.
28. Qin, H., Srinivasula, S. M., Wu, G., Fernandes-Alnemri, T., Alnemri, E. S. & Shi, Y. (1999). Structural basis of procaspase-9 recruitment by the apoptotic protease-activating factor 1. *Nature*, **399**, 549–557.
29. Hill, J. M., Morisawa, G., Kim, T., Huang, T., Wei, Y. & Werner, M. H. (2004). Identification of an expanded binding surface on the FADD death domain responsible for interaction with CD95/Fas. *J. Biol. Chem.* **279**, 1474–1481.
30. Hendrickson, W. A., Horton, J. R. & LeMaster, D. M. (1990). Selenomethionyl proteins produced for analysis by multiwavelength anamalous diffraction (MAD): a vehicle for direct determination of three dimensional structure. *EMBO J.* **9**, 1665–1672.
31. Otwinowski, Z. (1990). *DENZO Data Processing Package*, Yale University, New Haven, CT.
32. Terwilliger, T. (2004). SOLVE and RESOLVE:automated structure solution, density modification and model building. *J. Synchrotron Radiat.* **11**, 49–52.
33. Jones, T. A., Zou, J.-Y., Cowan, S. W. & Kjeldgaard, M. (1991). Improved methods for building models in electron density maps and the location of errors in those models. *Acta Crystallg. sect. A*, **47**, 110–119.
34. Brunger, A. T., Adams, P. D., Clore, G. M., DeLano, W. L., Gros, P., Grosse-Kunstleve, R. W. *et al.* (1998). Crystallography & NMR system: a new software suite for macromolecular structure determination. *Acta Crystallog. sect. D*, **54**, 905–921.

35. Evans, S. V. (1993). SETOR: hardware-lighted three-dimensional solid model representations of macromolecules. *J. Mol. Graph.* **11**, 134–138.
36. Kraulis, P. J. (1991). MOLSCRIPT: a program to produce both detailed and schematic plots of protein structures. *J. Appl. Crystallog.* **24**, 946–950.
37. Merritt, E. A. & Murphy, M. E. (1994). Raster3D version 2.0. A program for photorealistic molecular graphics. *Acta Crystallog. sect. D*, **50**, 869–873.
38. Nicholls, A., Sharp, K. A. & Honig, B. (1991). Protein folding and association: insights from the interfacial and thermodynamic properties of hydrocarbons. *Proteins: Struct. Funct. Genet.* **11**, 281–296.

Edited by I. Wilson

(Received 1 December 2005; received in revised form 21 December 2005; accepted 27 December 2005)
Available online 11 January 2006